

Edyta Pięciorak  [orcid.org/0000-0001-6664-9927](https://orcid.org/0000-0001-6664-9927)  
epiec@agh.edu.pl

Henryk Ciurej  [orcid.org/0000-0003-4017-6185](https://orcid.org/0000-0003-4017-6185)

Michał Betlej  [orcid.org/0000-0001-7631-0134](https://orcid.org/0000-0001-7631-0134)

AGH University, Faculty of Mining and Geoengineering, Department of Geomechanics,  
Civil Engineering and Geotechnology

Marek Piekarczyk  [orcid.org/0000-0003-0566-4749](https://orcid.org/0000-0003-0566-4749)

Faculty of Civil Engineering, Cracow University of Technology

THE DETERMINATION OF MOMENT RESISTANCE FOR A LINER TRAY  
RESTRAINED BY SHEETING ACCORDING TO EUROPEAN STANDARD  
PN-EN 1993-1-3

---

WYZNACZANIE NOŚNOŚCI PRZY ZGINANIU KASETY ŚCIENNEJ  
USZTYWNIONEJ POSZYCIEM W UJĘCIU NORMY EUROPEJSKIEJ  
PN-EN 1993-1-3

**Abstract**

The paper presents an example of the determination of moment resistance for a liner tray restrained by sheeting according to the rules given in standard PN-EN 1993-1-3 [12].

**Keywords:** liner tray, moment resistance, channel-type section, effective cross section

**Streszczenie**

W artykule przedstawiono przykład obliczeniowy wyznaczania nośności przy zginaniu kasety ściennej usztywnionej poszyciem wg wytycznych normy PN-EN 1993-1-3 [12].

**Słowa kluczowe:** kaseata ścienna, nośność przy zginaniu, przekrój ceowy, przekrój współpracujący

## 1. Introduction

Light gauge steel cassettes, also often named liner trays, are made from cold-formed C-shaped steel sections, typically with the geometry shown in Fig. 1. The idea of a cassette wall construction has its origins in an invention by Baehre in Stockholm in the late 1960s [3]. Extensive research on the behavior of steel cassettes under loading was conducted at that time by Baehre et al. [1, 2, 11, 19, 20] and later by Davies et al. [5–7]. Their results formed the basis of the design clauses given in Eurocode 3, Part 1–3 [4, 12].

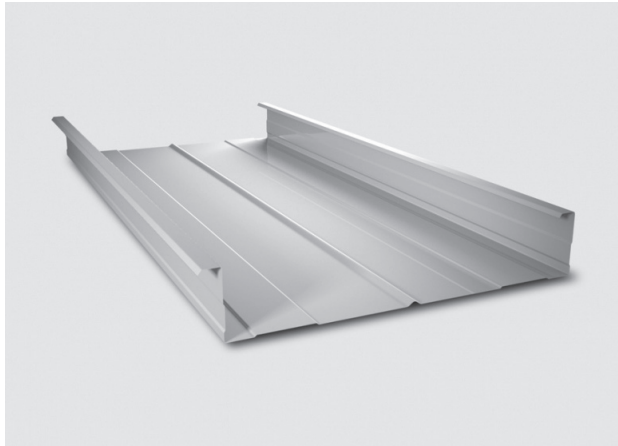


Fig. 1. Example of a liner tray [9]

At present, cassette sections are widely used, mainly for industrial buildings and warehouses as an alternative to traditional wall construction using beams. Figure 2 presents an example of the usage of liner trays as wall members.

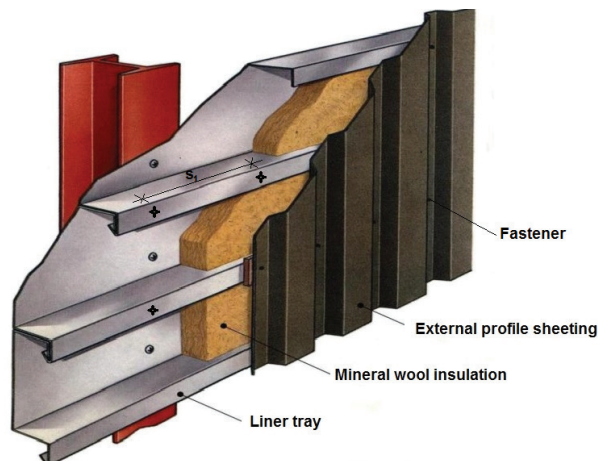


Fig. 2. Example of using liner trays in wall cladding system [10]

Cassette walls are subjected to three primary load combinations: axial load, bending, and shear [8]. This paper presents the design procedures (determination of moment resistance) for trays subjected to bending resulting from wind pressure and suction according to the rules given in the standard PN-EN 1993-1-3 [12].

The behaviour of a cassette section under bending is characterised by the usual relationships that apply to all thin-walled cold-formed sections. However, the design of a cassette with a narrow flange which is under compression (caused by e.g. wind pressure), is a particularly complicated problem because the following four effects should be considered here: local buckling of the web and narrow flanges; distortional buckling of the narrow flange and edge stiffener assemblies; flange curling of the wide flange which is under tension; the effects of shear lag. If the wide flange of a cassette subjected to bending is under compression (caused by e.g. wind suction), the narrow flange and edge stiffener assemblies are under tension and do not buckle. Bending behaviour is dominated by local buckling of the wide flange. PN-EN 1993-1-3 [12] does not propose any special treatment for the interaction of flange curling that occurs in the wide flange under compression and local buckling. This seems to be too difficult; instead, it is suggested in the standard that the conventional effective width procedure should be used but with the material factor  $\gamma_{M0}$  increased to 1.25 [8].

## 2. Typical geometry of liner trays

The elements of a typical cassette section have two narrow flanges ( $b_{f1}, b_{f2}$ ), two webs ( $h_1, h_2$ ) with intermediate stiffeners ( $h_{u3}$ ), one wide flange ( $b_u$ ) with intermediate stiffeners ( $h_{u1}$  and  $h_{u2}$ ), and two edge stiffeners ( $c$ ), as shown in Fig. 3.

The analytical calculations for the moment resistance of a liner tray were performed with the use of Mathcad 14 [15] for the cross section presented in Fig. 3 [9] and the static scheme as a simply supported beam shown in Fig. 4.

The effective section properties of this element were determined in AutoCAD program [14].

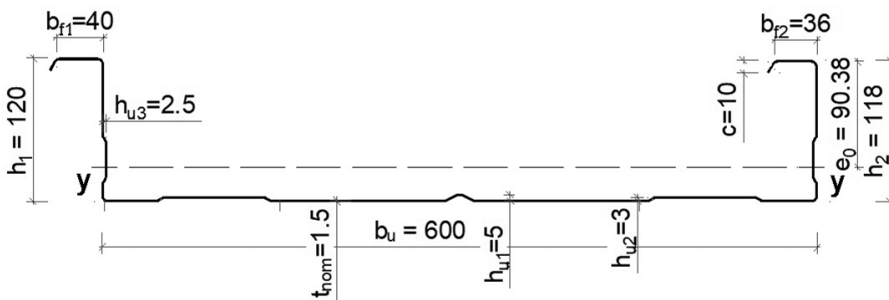


Fig. 3. The geometry of a 600/120 wall cassette

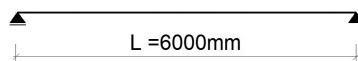


Fig. 4. The static scheme of a 600/120 wall cassette

### 3. Calculation of the thickness of the designed liner tray

After applying formula (3.3c) in [12]:

$$t = t_{cor} = t_{nom} - t_{metallic} = 1.5 - 0.04 = 1.46 \text{ mm}, \quad (1)$$

where:

- $t$  – core thickness of steel material before cold forming,
- $t_{nom}$  – nominal sheet thickness after cold forming (inclusive of zinc or other metallic coating)  $t_{nom} = 1.5 \text{ mm}$
- $t_{cor}$  – the nominal thickness minus zinc or other metallic coating
- $t_{metallic}$  – the thickness of the metallic coating (for the usual Z275 zinc coating,  $t_{zinc} = 0.04 \text{ mm}$ )

### 4. Verification of the standard geometric proportions of the liner tray

The recommendations for the design given in PN-EN 1993-1-3 [12] can be applied to cross sections for which width-to-thickness ratios are within the following ranges as adopted from Table 5.1 in [12] (see Table 1):

Table 1. Maximum width-to-thickness ratios

Element of cross section (see Fig. 3)	Geometric proportions (see Fig. 3)	Maximum value (see Tab. 5.1 in [12])
narrow flange $b_{f1}$	$b_{f1}/t = 40 \text{ mm}/1.46 \text{ mm}$ $b_{f1}/t = 27.40$	60
narrow flange $b_{f2}$	$b_{f2}/t = 36 \text{ mm}/1.46 \text{ mm}$ $b_{f2}/t = 24.66$	60
edge stiffeners $c$	$c/t = 10 \text{ mm}/1.46 \text{ mm}$ $c/t = 6.85$	50
wide flange $b_u$	$b_u/t = 600 \text{ mm}/1.46 \text{ mm}$ $b_u/t = 410.96$	500
web $h_1$	$h_1/t = 120 \text{ mm}/1.46 \text{ mm}$ $h_1/t = 82.19$	$500 \cdot (\sin \phi) = 500 \cdot (\sin 90^\circ) = 500$
web $h_2$	$h_2/t = 118 \text{ mm}/1.46 \text{ mm}$ $h_2/t = 80.82$	$500 \cdot (\sin \phi) = 500 \cdot (\sin 90^\circ) = 500$

where:

$\phi$  – angle between the wide flange and the web.

In order to provide sufficient stiffness and to avoid primary buckling of the stiffener itself, the size of the stiffener according to (5.2a) in [12] should be within the following range:

$$0.2 < \frac{c}{b} = \frac{10}{40} = 0.25 < 0.6, \quad (2)$$

where, according to Fig. 3:  $c = 10$  mm,  $b = b_{f1} = 40$  mm for the left end

$$0.2 < \frac{c}{b} = \frac{10}{36} = 0.28 < 0.6, \quad (3)$$

and  $c = 10$  mm,  $b = b_{f2} = 36$  mm for the right end.

If  $c/b < 0.2$ , the lip should be ignored ( $c = 0$ ).

It can be concluded that the geometric proportions of this liner tray are appropriate and allow the use of standard PN-EN-1993-1-3 [12].

The moment resistance of a liner tray may be obtained using 10.2 in [12] provided that the geometric properties are within the range given in Table 10.6 [12] and the depths  $h_{u1}$  and  $h_{u2}$  (see Fig. 3) of the corrugations of the wide flange do not exceed  $h/8$ , where  $h$  ( $h_1$ ,  $h_2$ ) is the overall depth of the liner tray (see Fig. 3). The range of validity of the design procedures according to 10.2 [12] is as follows (see Table 2):

Table 2. The range of validity of the design procedures according to 10.2 [12] in dependence on the geometry of a cross section

Minimum value	Dimensions and geometrical proportions (see Fig. 3)	Maximum value
0.75 mm	$t_{nom} = 1.5$ mm	1.5 mm
30 mm	$b_{f1} = 40$ mm	60 mm
30 mm	$b_{f2} = 36$ mm	60 mm
60 mm	$h_1 = 120$ mm	200 mm
60 mm	$h_2 = 118$ mm	200 mm
300 mm	$b_u = 600$ mm	600 mm
—	$I_a/b_u = 1932 \text{ mm}^4/600 \text{ mm}$ $I_a/b_u = 3.22 \text{ mm}^4/\text{mm}$ (see Fig. 5)	$10 \text{ mm}^4/\text{mm}$
—	$s_1 = 210$ mm (see Fig. 2)	1000 mm
—	$h_{u1} = 5$ mm	$h_1/8 = 120 \text{ mm}/8 = 15 \text{ mm}$ $h_2/8 = 118 \text{ mm}/8 = 14.75 \text{ mm}$ (see Fig. 3)
—	$h_{u2} = 3$ mm	$h_1/8 = 120 \text{ mm}/8 = 15 \text{ mm}$ $h_2/8 = 118 \text{ mm}/8 = 14.75 \text{ mm}$ (see Fig. 3)

where:

- $s_1$  – the spacing of fasteners in the narrow flanges (see Fig. 2),
- $I_a$  – the second moment of area of the wide flange  $b_u$ , about its own centroid (a-a), calculated with use of AutoCAD [14]
- $I_a = 1,932 \text{ mm}^4$  (see Fig. 5).

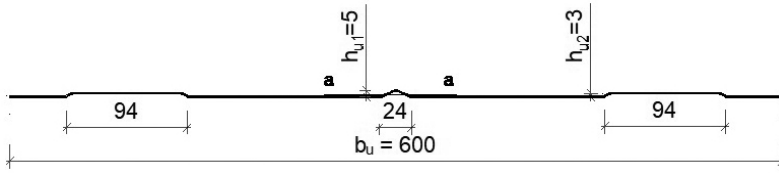


Fig. 5. The geometry of the wide flange of the liner tray

## 5. Design procedures for liner trays restrained by sheeting

### 5.1. Determination of moment resistance of a liner tray section with its wide flange under compression

The moment resistance  $M_{c,Rd}$  of liner trays restrained by sheeting may be obtained as follows, after applying formula (10.19) in [12]:

$$M_{c,Rd} = \frac{0.8 \cdot W_{eff,min} \cdot f_{yb}}{\gamma_{MO}} = \frac{0.8 \cdot 19101 \cdot 320}{1.0} = 4,890 \text{ kNm}, \quad (4)$$

where:

- $f_{yb}$  – the basic yield strength 320 N/mm<sup>2</sup>,
- $\gamma_{MO}$  – the partial safety factor equal to 1.0,
- $W_{eff,min}$  – the minimum effective section modulus calculated as follows:

$$W_{eff,min} = \frac{I_{y,eff}}{z_c} = \frac{1177987}{61.67} = 19,101 \text{ mm}^3, \quad (5)$$

and

$$W_{eff,min} = 19,101 \text{ mm}^3 \leq \frac{I_{y,eff}}{z_t} = \frac{1177987}{56.87} = 20,713 \text{ mm}^3, \quad (6)$$

where:

- $I_{y,eff}$  – the effective second moment of area (see Fig. 7 and 5.1.1) about the y-y axis,  $I_{y,eff} = 1,177,987 \text{ mm}^4$ ,
- $z_c$  – the distance from the effective centroidal axis to the system line of the compression wide flange (see Fig. 7),  $z_c = \max(z_{c1}, z_{c2}) = 61.67 \text{ mm}$ ,
- $z_t$  – the distance from the effective centroidal axis to the system line of the narrow flange in tension (see Fig. 7),  $z_t = \max(z_{t1}, z_{t2}) = 56.87 \text{ mm}$ .

### 5.1.1. Determination of the effective width $b_{eff}$ of the wide flange under compression

The relative slenderness  $\bar{\lambda}_p$  according to (4.2) in [13] is:

$$\bar{\lambda}_p = \frac{\bar{b}/t}{28,4\varepsilon\sqrt{k_\sigma}} = \frac{596,6/1,46}{28,4 \cdot 0,857 \cdot \sqrt{4}} = 8,395, \quad (7)$$

where, according to Fig. 6:  $\bar{b} = b_{pu} = 596,6$  mm,  $t = 1,46$  mm, local buckling factor  $k_\sigma = 4,0$

for  $\psi = \frac{\sigma_2}{\sigma_1} = 1$  (uniform compression in the flange  $b_{pu}$ ),  $\varepsilon = \sqrt{\frac{235}{f_{yb}}} = \sqrt{\frac{235}{320}} = 0,857$ .

The reduction factor  $\rho$  of effective width according to (4.2) in [13] is:

$$\rho = \frac{\bar{\lambda}_p - 0,055 \cdot (3 + \psi)}{\bar{\lambda}_p^2} = \frac{8,395 - 0,055 \cdot (3 + 1)}{8,395^2} = 0,116 \leq 1,0, \quad (8)$$

for:

$$\bar{\lambda}_p = 8,395 > 0,5 + \sqrt{0,085 - 0,055\psi} = 0,5 + \sqrt{0,085 - 0,055 \cdot 1,0} = 0,673. \quad (9)$$

The effective width  $b_{u,eff}$  of the wide flange  $b_{pu}$  can be calculated according to Table 4.1 in [13] as follows:

$$b_{u,eff} = \rho \cdot \bar{b} = 0,116 \cdot 596,6 = 69,20 \text{ mm}, \quad (10)$$

where, according to Fig. 6:  $\bar{b} = b_{pu} = 596,6$  mm and formula (8)  $\rho = 0,116$ .

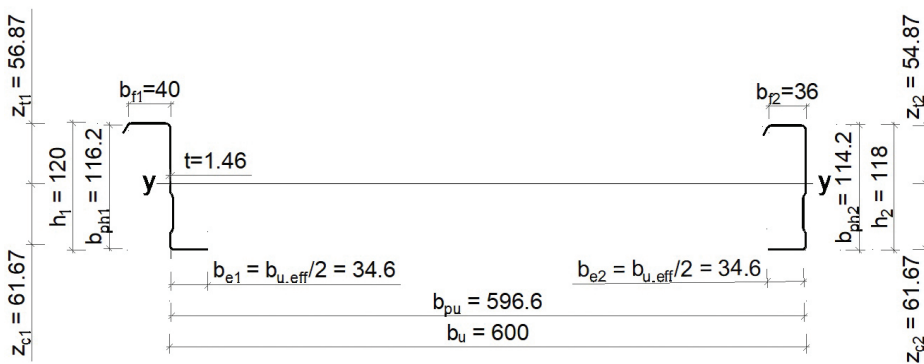


Fig. 6. Effective cross section of the wide flange under compression and the entire cross sections of the webs of a 600/120 wall cassette

The initial values of the effective widths  $b_{e1}$  and  $b_{e2}$  shown in Fig. 6 should be determined according to Table 4.1 in [13] for a doubly supported wide flange  $b_{pu}$  as follows:

$$b_{e1} = b_{e2} = 0.5 \cdot b_{u,eff} = 0.5 \cdot 69.2 = 34.6 \text{ mm.} \quad (11)$$

### 5.1.2. Determination of effective width $h_{eff}$ of the web under bending

The relative slenderness  $\bar{\lambda}_p$  according to (4.2) in [13] is:

**For web  $h_1$ :**

$$\bar{\lambda}_p = \frac{\bar{b}/t}{28,4\epsilon\sqrt{k_\sigma}} = \frac{116.2/1.46}{28,4 \cdot 0.857 \cdot \sqrt{21.93}} = 0.7, \quad (12)$$

where, according to Fig. 6:  $\bar{b} = b_{ph1} = 116.2 \text{ mm}$ ,  $t = 1.46 \text{ mm}$ ,  $\epsilon = \sqrt{\frac{235}{f_{yb}}} = \sqrt{\frac{235}{320}} = 0.857$ , the value of  $k_\sigma$  may be calculated according to Table 4.1 [13] is as follows:

$$k_\sigma = 7.81 - 6.29\psi + 9.78\psi^2 = 7.81 - 6.29 \cdot (-0.92) + 9.78 \cdot (-0.92)^2 = 21.93, \quad (13)$$

for:

$$0 > \psi = -0.92 > -1, \quad (14)$$

with:

$$\psi = \frac{\sigma_2}{\sigma_1} = -\frac{56.87}{61.67} = -0.92, \quad (15)$$

where, according to Fig. 6:  $\sigma_2 = z_{t1} = 56.87 \text{ mm}$  and  $\sigma_1 = z_{c1} = 61.67 \text{ mm}$ .

The reduction factor  $\rho$  of the effective width according to (4.2) in [13] is as follows:

$$\rho = 1.0, \quad (16)$$

for:

$$\bar{\lambda}_p = 0.7 < 0.5 + \sqrt{0.085 - 0.055\psi} = 0.5 + \sqrt{0.085 - 0.055 \cdot (-0.92)} = 0.87. \quad (17)$$

The web is fully effective because the reduction factor of the effective width is  $\rho = 1.0$ . The effective width  $h_{eff}$  of the web can be calculated according to Table 4.1 in [13] is as follows:

$$h_{eff} = \rho \cdot b_c = 1.0 \cdot 61.67 = 61.67 \text{ mm}, \quad (18)$$

where, according to Fig. 6:  $b_c = z_{c1} = 61.67 \text{ mm}$  and formula (16)  $\rho = 1.0$ .

The initial values of the effective widths  $h_{e1}$  and  $h_{e2}$  shown in Fig. 7 should be determined according to Table 4.1 in [13] for a doubly supported web as follows:

$$h_{e1} = 0.4 \cdot h_{eff} = 0.4 \cdot 61.67 = 24.67 \text{ mm}, \quad (19)$$

$$h_{e2} = 0.6 \cdot h_{eff} = 0.6 \cdot 61.67 = 37 \text{ mm}. \quad (20)$$



The analytical calculations for the web  $h_2$  were performed in the same manner as for web  $h_1$ . The initial values of the effective widths  $h_{e1} = 24.67$  mm and  $h_{e2} = 37$  mm are the same as the values calculated before (see Fig. 7).

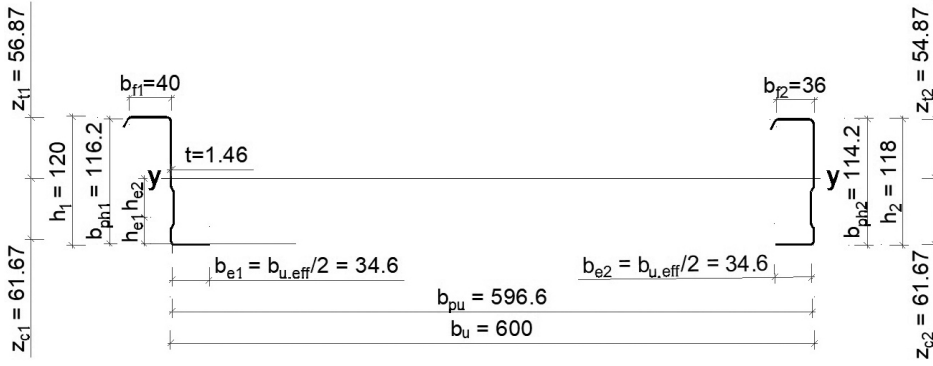


Fig. 7. Effective cross section of the liner tray of a 600/120 wall cassette

The effective moment of inertia for a liner tray (see Fig. 7) with its wide flange under compression about the y-y axis is  $I_{y,eff} = 1,177,987 \text{ mm}^3$ .

### 5.1.3. The effects of shear lag

According to (10.2.2.2 (2)) in [12], the effects of shear lag may be neglected here because:

$$\frac{L}{b_{u,eff}} = \frac{6000}{69.20} = 86.71 \geq 25, \quad (21)$$

where, according to Fig. 4:  $L = 6000$  mm and according to formula (10),  $b_{u,eff} = b_{eff} = 69.20$  mm.

### 5.2. Determination of moment resistance of a liner tray section with its narrow flange under compression

The buckling moment resistance  $M_{b,Rd}$  of linear trays restrained by sheeting may be obtained as follows, according to formula 10.21 in [12]:

$$M_{b,Rd} = \frac{0.8 \cdot \beta_b \cdot W_{eff,com} \cdot f_{yb}}{\gamma_{M0}} = \frac{0.8 \cdot 1.0 \cdot 22725.4 \cdot 320}{1.0} = 5.82 \text{ kNm}, \quad (22)$$

and

$$M_{b,Rd} \leq \frac{0.8 \cdot W_{eff,t} \cdot f_{yb}}{\lambda_{M0}} = \frac{0.8 \cdot 47537.1 \cdot 320}{1.0} = 12.17 \text{ kNm}, \quad (23)$$

where:

$f_{yb}$  – the basic yield strength 320 N/mm<sup>2</sup>,

- $\gamma_{M0}$  – the partial safety factor equal to 1.0,
- $\beta_b$  – the correlation factor that depends on the longitudinal spacing of fasteners supplying lateral restraint to the narrow flanges  $s_1$  (see Fig. 2) for  $s_1 = 210$  mm  $\leq 300$  mm  $\beta_b = 1.0$  and for  $300$  mm  $\leq s_1 \leq 1000$  mm:  $\beta_b = 1.15 \cdot s_1 / 2000$ ,
- $W_{eff,com}$  – the effective section modulus for the maximum compressive stress in a cross section is as follows:

$$W_{eff,com} = \frac{I_{y,eff}}{z_c} = \frac{1822575.8}{80.20} = 22,725.4 \text{ mm}^3, \quad (24)$$

- $W_{eff,t}$  – the effective section modulus for the maximum tensile stress in a cross section is as follows:

$$W_{eff,t} = \frac{I_{y,eff}}{z_t} = \frac{1822575.8}{38.34} = 47,537.1 \text{ mm}^3, \quad (25)$$

where:

- $I_{y,eff}$  – the effective second moment of area (see Fig. 12 and 5.2.1) about the y-y axis,  $I_{y,eff} = 1,822,575.8 \text{ mm}^3$ ,
- $z_c$  – the distance from the effective centroidal axis to the system line of the wide flange under compression (see Fig. 12),  $z_c = \max(z_{c1}, z_{c2}) = 80.20$  mm,
- $z_t$  – the distance from the effective centroidal axis to the system line of the narrow flange in tension (see Fig. 12),  $z_t = \max(z_{t1}, z_{t2}) = 38.34$  mm.

### 5.2.1. Determination of the effective width $b_{u,eff}$ of the wide flange under tension

The effective width  $b_{u,eff}$  of the wide flange under tension (see Fig. 8) allowing for possible flange curling according to (10.20) in [12] is given by:

$$b_{u,eff} = \frac{53.3 \cdot 10^{10} \cdot e_0^2 \cdot t^3 \cdot t_{eq}}{h \cdot L \cdot b_u^3} = \frac{53.3 \cdot 10^{10} \cdot 90.38^2 \cdot 1.46^3 \cdot 3.38}{120 \cdot 6000 \cdot 600^3} = 294.55 \text{ mm}, \quad (26)$$

where, according to Fig. 4:  $L = 6000$  mm and according to Fig. 3:  $e_0 = 90.38$  mm,  $b_u = 600$  mm,  $t = 1.46$  mm (see formula (1)). The value of  $t_{eq}$  may be calculated according to (10.2.2.2 (1)) in [12] as follows:

$$t_{eq} = \left( \frac{12 \cdot I_a}{b_u} \right)^{\frac{1}{3}} = \left( \frac{12 \cdot 1932}{6000} \right)^{\frac{1}{3}} = 3.38, \quad (27)$$

where, according to Fig. 3:  $b_u = 600$  mm, and the second moment of area of the wide flange about its own centroid a-a  $I_a$ , calculated with the use of AutoCAD [14], is equal to  $1,932 \text{ mm}^4$  (see Fig. 5).

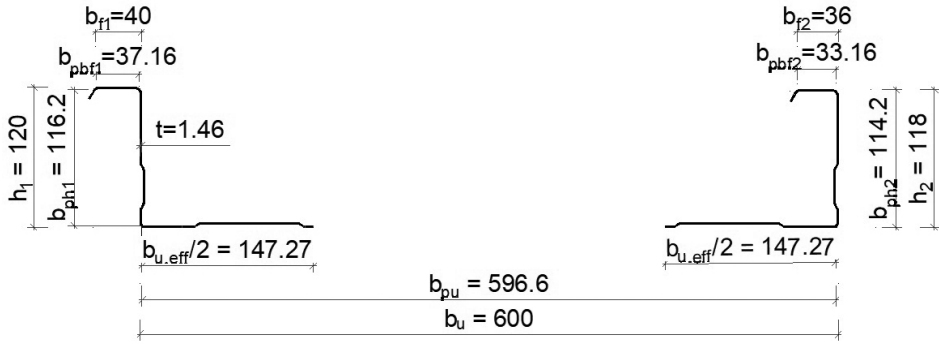


Fig. 8. Effective width  $b_{u,eff}$  of the wide flange of a 600/120 wall cassette under tension

### 5.2.2. Determination of effective width $b_{eff}$ of the narrow flange under compression

The relative slenderness  $\bar{\lambda}_p$  according to (4.2) in [13] is:

**For the narrow flange  $b_{f1}$ :**

$$\bar{\lambda}_p = \frac{\bar{b}/t}{28,4\varepsilon\sqrt{k_\sigma}} = \frac{37.16/1.46}{28,4 \cdot 0.857 \cdot \sqrt{4}} = 0.523, \quad (28)$$

where, according to Fig. 8:  $\bar{b} = b_{pbf1} = 37.16$  mm,  $t = 1.46$  mm, local buckling factor  $k_\sigma = 4.0$

for  $\psi = \frac{\sigma_2}{\sigma_1} = 1$  (uniform compression in the flange  $b_{f1}$ ),  $\varepsilon = \sqrt{\frac{235}{f_{yb}}} = \sqrt{\frac{235}{320}} = 0.857$ .

The reduction factor  $\rho$  of the effective width according to (4.2) in [13] is:

$$\rho = 1.0, \quad (29)$$

for:

$$\bar{\lambda}_p = 0.523 < 0.5 + \sqrt{0.085 - 0.055\psi} = 0.5 + \sqrt{0.085 - 0.055 \cdot 1.0} = 0.673. \quad (30)$$

The narrow flange  $b_{f1}$  is fully effective because the reduction factor of the effective width  $\rho = 1.0$ . The effective width  $b_{eff}$  of the narrow flange  $b_{f1}$  can be calculated according to Table 4.1 in [13] as follows:

$$b_{eff} = \rho \cdot \bar{b} = 1.0 \cdot 37.16 = 37.16 \text{ mm}, \quad (31)$$

where, according to Fig. 8:  $\bar{b} = b_{pbf1} = 37.16$  mm and formula (29)  $\rho = 1.0$ .

The initial values of the effective widths  $b_{e1}$  and  $b_{e2}$  shown in Fig. 9 should be determined with accordance to Table 4.1 in [13] for a doubly supported wide flange  $b_{pbf1}$  as follows:

$$b_{1,e1} = b_{1,e2} = 0.5 \cdot b_{eff} = 0.5 \cdot 37.16 = 18.58 \text{ mm}. \quad (32)$$

**For the narrow flange  $b_{f2}$ :**

$$\bar{\lambda}_p = \frac{\bar{b}/t}{28,4\epsilon\sqrt{k_\sigma}} = \frac{33.16/1.46}{28,4 \cdot 0.857 \cdot \sqrt{4}} = 0.467, \quad (33)$$

where, according to Fig. 8:  $\bar{b} = b_{pbf2} = 33.16$  mm,  $t = 1.46$  mm, local buckling factor  $k_\sigma = 4.0$

for  $\psi = \frac{\sigma_2}{\sigma_1} = 1$  (uniform compression in the flange  $b_{f2}$ ),  $\epsilon = \sqrt{\frac{235}{f_{yb}}} = \sqrt{\frac{235}{320}} = 0.857$ .

The reduction factor  $\rho$  of the effective width according to (4.2) in [13] is:

$$\rho = 1.0, \quad (34)$$

for:

$$\bar{\lambda}_p = 0.467 < 0.5 + \sqrt{0.085 - 0.055\psi} = 0.5 + \sqrt{0.085 - 0.055 \cdot 1.0} = 0.673. \quad (35)$$

The narrow flange  $b_{f2}$  is fully effective because the reduction factor of effective width  $\rho = 1.0$ . The effective width  $b_{eff}$  of the narrow flange  $b_{f2}$  can be calculated according to Table 4.1 in [13] as follows:

$$b_{eff} = \rho \cdot \bar{b} = 1.0 \cdot 33.16 = 33.16 \text{ mm}, \quad (36)$$

where, according to Fig. 8:  $\bar{b} = b_{pbf2} = 33.16$  mm and formula (34)  $\rho = 1.0$ .

The initial values of the effective widths  $b_{e1}$  and  $b_{e2}$  shown in Fig. 10 should be determined according to Table 4.1 in [13] for a doubly supported wide flange  $b_{pbf2}$  as follows:

$$b_{2,e1} = b_{2,e2} = 0.5 \cdot b_{eff} = 0.5 \cdot 33.16 = 16.58 \text{ mm}. \quad (37)$$

### 5.2.3. Determination of effective area of the edge stiffener of the narrow flange under compression

Initial values of the effective width  $c_{eff}$  shown in Fig. 9 and Fig. 10 should be obtained for a single edge fold stiffener according to (5.13a) in [12] as follows:

$$c_{eff} = \rho \cdot b_{p,c} = 1.0 \cdot 11 = 11 \text{ mm}, \quad (38)$$

where, according to Fig. 9 for the narrow flange  $b_{f1}$  and Fig. 10 for the narrow flange,  $b_{f2}$ :  $b_{p,c} = 11$  mm and according to formula (42),  $\rho = 1.0$ .

The relative slenderness  $\bar{\lambda}_p$  according to (4.2) in [13] is:

**For the narrow flange  $b_{f1}$  and  $b_{f2}$ :**

$$\bar{\lambda}_p = \frac{\bar{b}/t}{28,4\epsilon\sqrt{k_\sigma}} = \frac{11/1.46}{28,4 \cdot 0.857 \cdot \sqrt{0.5}} = 0.438, \quad (39)$$

for:

where, according to Fig. 9:  $b_p = b_{pbf1} = 37.16$  mm  
and for:

where, according to Fig. 10:  $b_p = b_{pbf2} = 33.16 \text{ mm}$ .

$$\rho=1.0, \quad (42)$$

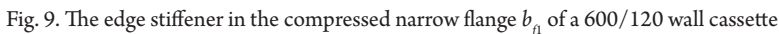
for :

The geometric properties of the stiffener determined in the AutoCAD program [14]:

**For the narrow flange  $b_{fl}$  (see Fig. 9):**

$$A_{s1} = 42.83 \text{ mm}^2$$

$$I_{s1} = 342.89 \text{ mm}^4$$



The relative slenderness  $\bar{\lambda}_d$  according to (5.12d) in [12] is:

where:

- $f_{yb}$  – the basic yield strength 320 N/mm<sup>2</sup>,  
 $\sigma_{cr,s}$  – the critical stress in the edge stiffener according to (5.15) in [12] is as follows:

$$\sigma_{cr,s} = \frac{2 \cdot \sqrt{K \cdot E \cdot I_s}}{A_s} = \frac{2 \cdot \sqrt{1.05 \cdot 210000 \cdot 342.89}}{42.83} = 406 \text{ MPa}, \quad (45)$$

where:

- $A_s$  – the effective cross-sectional area of the edge stiffener,  $A_s = A_{s1}$ ,
- $I_s$  – the effective second moment of area of the stiffener, taken as that of its effective area  $A_{s1}$  about the centroidal axis a-a of its effective cross section,  $I_s = I_{s1}$  (see Fig. 9),
- $K$  – the spring stiffness of the edge stiffener per unit length according to (5.10b) in [12] as follows:

$$K = \frac{Et^3}{4 \cdot (1-\nu^2)} \cdot \frac{1}{b_1^2 \cdot h_w + b_1^3} = \frac{210 \cdot 10^3 \cdot 1.46^3}{4 \cdot (1-0.3^2) \cdot 33.77^2 \cdot 116.2 + 33.77^3} = 1.05 \text{ MPa}, \quad (46)$$

where:

- $b_1$  – the distance according to Fig. 9,  $b_1 = 33.77$  mm,
- $h_w$  – the web depth,  $h_w = b_{ph1} = 116.2$  mm (see Fig. 6),
- $\nu$  – the Poisson's ratio,  $\nu = 0.3$ .

For profiles with one flange under tension (when the element is bending about y-y axis)  $k_f = 0$  in (5.10b) in [12].

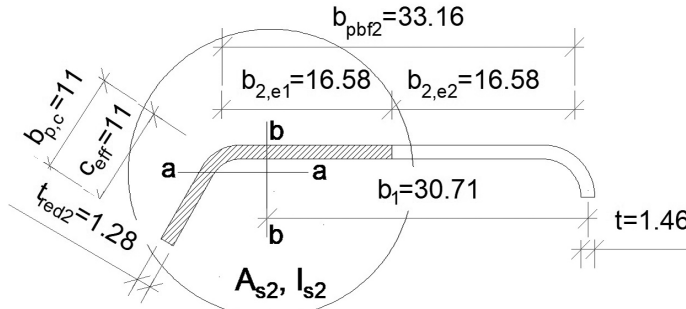


Fig. 10. The edge stiffener in the compressed narrow flange  $b_{p2}$  of a 600/120 wall cassette

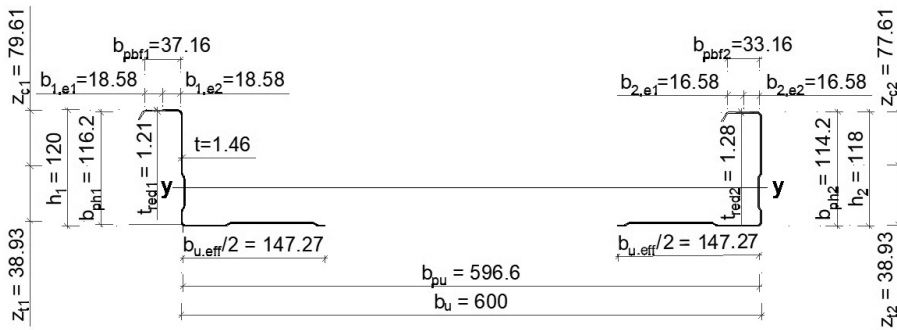


Fig. 11. Effective cross section of the narrow flange under compression and the entire cross sections of the webs of a 600/120 wall cassette

The reduction factor  $\chi_d$  for the distortional buckling resistance (flexural buckling of a stiffener) according to (5.12b) in [12] is:

$$\chi_d = 1.47 - 0.723 \cdot \bar{\lambda}_d = 1.47 - 0.723 \cdot 0.888 = 0.828 < 1.0, \quad (47)$$

for:

$$0.65 < \bar{\lambda}_d = 0.888 < 1.38. \quad (48)$$

The reduced thickness  $t_{red1}$  of the edge stiffener in the compressed flange  $b_{f1}$  is:

$$t_{red1} = \chi_d \cdot t = 0.828 \cdot 1.46 = 1.21 \text{ mm}. \quad (49)$$

The analytical calculations for narrow flange  $b_{f2}$  (see Fig. 10) were performed in the same manner as for narrow flange  $b_{f1}$ . The reduction factor  $\chi_d$  for the distortional buckling resistance of a stiffener according to (5.12b) in [12] is  $\chi_d = 0.88$ .

The reduced thickness  $t_{red2}$  of the edge stiffener in the compressed flange  $b_{f2}$  is:

$$t_{red2} = \chi_d \cdot t = 0.88 \cdot 1.46 = 1.28 \text{ mm}. \quad (50)$$

$$A_{s2} = 39.91 \text{ mm}^2,$$

$$I_{s2} = 332.66 \text{ mm}^4.$$

#### 5.2.4. Determination of effective depth of the webs $h_1$ and $h_2$ under bending

The relative slenderness  $\bar{\lambda}_p$  according to (4.2) in [13] is:

**For web  $h_1$ :**

$$\lambda_p = \frac{\bar{b}/t}{28,4\varepsilon\sqrt{k_\sigma}} = \frac{116.2/1.46}{28,4 \cdot 0.857 \cdot \sqrt{13.23}} = 0.899, \quad (51)$$

where, according to Fig. 6:  $\bar{b} = b_{ph1} = 116.2 \text{ mm}$ ,  $t = 1.46 \text{ mm}$ ,  $\varepsilon = \sqrt{\frac{235}{f_{yb}}} = \sqrt{\frac{235}{320}} = 0.857$ , the value of  $k_\sigma$  may be calculated according to Table 4.1 [13] as follows:

$$k_\sigma = 7.81 - 6.29\psi + 9.78\psi^2 = 7.81 - 6.29 \cdot (-0.49) + 9.78 \cdot (-0.49)^2 = 13.23, \quad (52)$$

for:

$$0 > \psi = -0.49 > -1, \quad (53)$$

with:

$$\psi = \frac{\sigma_2}{\sigma_1} = -\frac{38.93}{79.61} = -0.49, \quad (54)$$

where, according to Fig. 11:  $\sigma_2 = z_{t1} = 38.93 \text{ mm}$  and  $\sigma_1 = z_{c1} = 79.61 \text{ mm}$ .

The reduction factor  $\rho$  of effective width according to (4.2) in [13] is as follows:

$$\rho = \frac{\bar{\lambda}_p - 0.055 \cdot (3 + \psi)}{\bar{\lambda}_p^2} = \frac{0.899 - 0.055 \cdot (3 - 0.49)}{0.899^2} = 0.94, \quad (55)$$

for:

$$\bar{\lambda}_p = 0.899 > 0.5 + \sqrt{0.085 - 0.055\psi} = 0.5 + \sqrt{0.085 - 0.055 \cdot (-0.49)} = 0.835. \quad (56)$$

The effective width  $h_{eff}$  of the web can be calculated according to Table 4.1 in [13] as follows:

$$h_{eff} = \rho \cdot b_c = 0.94 \cdot 79.61 = 74.93 \text{ mm}, \quad (57)$$

where, according to Fig. 11:  $b_c = z_{c1} = 79.61 \text{ mm}$  and according to formula (55)  $\rho = 0.94$ .

The initial values of the effective widths  $h_{1,e1}$  and  $h_{1,e2}$  shown in Fig. 12 should be determined according to Table 4.1 in [13] for a doubly supported web as follows:

$$h_{1,e1} = 0.4 \cdot h_{eff} = 0.4 \cdot 74.93 = 29.97 \text{ mm}, \quad (58)$$

$$h_{1,e2} = 0.6 \cdot h_{eff} = 0.6 \cdot 74.93 = 44.96 \text{ mm}. \quad (59)$$

#### For web $h_2$ :

The analytical calculations for the web  $h_2$  were performed in the same manner as for web  $h_1$ . The initial values of the effective widths  $h_{2,e1} = 29.85 \text{ mm}$  and  $h_{2,e2} = 44.77 \text{ mm}$  are shown in Fig. 12.

The effective moment of inertia about y-y axis  $I_{y,eff}$  of a liner tray with its narrow flange under compression (see Fig. 12) is equal to  $1,822,575.8 \text{ mm}^3$ .

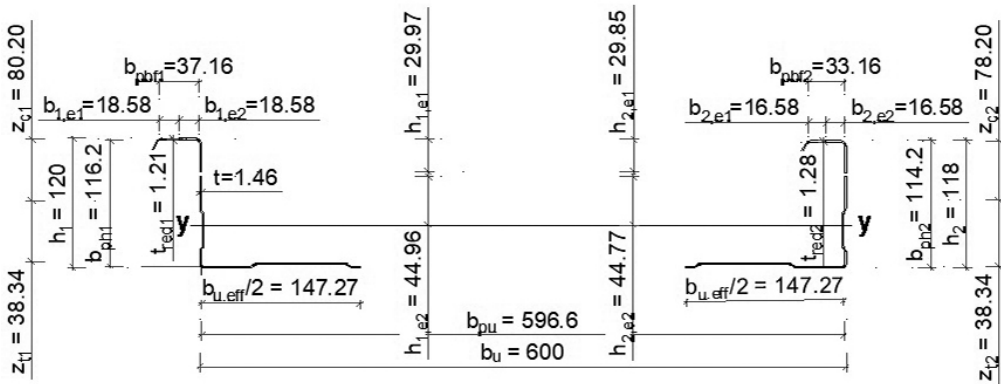


Fig. 12. Effective cross section of the narrow flange under compression of a 600/120 wall cassette

#### 5.2.5. The effects of shear lag

According to (10.2.2.2 (2)) in [12], the effects of shear lag have to be included if:

$$\frac{L}{b_{u,eff}} = \frac{6000}{294.55} = 20.37 < 25, \quad (60)$$

where, according to Fig. 4:  $L = 6000 \text{ mm}$  and according to formula (26),  $b_{u,eff} = 294.55 \text{ mm}$ .



The effective width  $b_{eff}$  for shear lag should be determined according to Section 3 in [13] with use of the relation:

$$b_{eff} = \beta \cdot b_0 = 0.984 \cdot 300 = 295.2 \text{ mm}, \quad (61)$$

where:

$b_0$  – is half the width of an internal element,  $b_0 = 300 \text{ mm}$ ,

$\beta$  – is the effective factor obtained for sagging bending, according to Table 3.1 in [13] as follows:

$$\beta = \frac{1}{1 + 6.4 \cdot \kappa^2} = \frac{1}{1 + 6.4 \cdot (0.05)^2} = 0.984, \quad (62)$$

for:

$$0.02 < \kappa = 0.05 \leq 0.7, \quad (63)$$

with:

$$\kappa = \frac{\alpha_0 \cdot b_0}{L_e} = \frac{1 \cdot 300}{6000} = 0.05, \quad (64)$$

where:

$\alpha_0$  – for the case without longitudinal stiffeners within the width  $b_0$ ,  $\alpha_0 = 1.0$ ,

$L_e$  – is the length between points of the zero bending moment (see 3.2.1(2) in [13],

$L_e = L = 6000 \text{ mm}$  (see Fig. 4).

The effective width  $b_{eff} = 295.20 \text{ mm}$  as a consequence of shear lag according to formula (61) is greater than the effective width  $b_{u,eff} = 294.55 \text{ mm}$  resulting from plate buckling according to formula (26), thus the effects of shear lag can be neglected.

## 6. Conclusion

This paper is a continuation of an analysis of some difficult cases of resistance calculations of sheeting for thin-wall constructions according to the rules given in the standard PN-EN 1993-1-3 (see [17, 18]).

This article presents an example of the determination of the resistance moment  $M_{b,Rd}$  of a 600/120 liner tray with a narrow flange under compression resulting from wind pressure and the resistance moment  $M_{c,Rd}$  of this liner tray with a wide flange under compression resulting from wind suction. The resistance in the case of the wind pressure on the wall of the liner trays  $M_{b,Rd}$  is 5.82 kNm. This is higher than the resistance of the linear tray  $M_{c,Rd}$  equal to 4.89 kNm in the case of wind suction.

The presented example proves that the analytical calculations according to PN-EN 1993-1-3 rules require good knowledge of linear tray performance.

*The contributions of E. Pięciórak, H. Ciurej and M. Betlej in the work were carried out as part of statutory research No. 11.11.100.197 AGH, WGiG, AGH University of Science and Technology in Cracow.*

## References

- [1] Baehre R., Buca J., *Die wirksame Breite des Zuggurtes von biegebeanspruchten Kassetten*, Stahlbau 55(9), 1986, 276–285.
- [2] Baehre R., *Zur Schubfeldwirkung und-Bemessung von Kassettenkonstruktionen*, Stahlbau 56(7), 1987, 197–202.
- [3] Davies J.M., *Cassette wall construction: Current Research and Practice*, Third International Conference on Advances in Steel Structures, Hong Kong, China, 9–11 December 2002, 57–68.
- [4] Davies J. M., *Residential buildings – Chapter 7: Light gauge metal structures Recent advances* (Ronald J. & Dubina D.), CISM International Centre for Mechanical Sciences, Vol. 455, 2005, 143–188.
- [5] Davies J.M., Dewhurst D.W., *The shear behaviour of thin-walled cassette sections infilled by rigid insulation*, Proceedings of International Conference on Experimental Model Research and Testing of Thin-Walled Structures, Prague, September 1997, 209–216.
- [6] Davies J. M., Frogos A. S., *The local shear buckling of thin-walled cassette infilled by rigid insulation – 1. Tests.*, Proceedings of 3<sup>rd</sup> European Conference on Steel Structures – Eurosteel 2002, Coimbra, Portugal, 19-20 September 2002, 669–678.
- [7] Davies J.M., Frogos A.S., *The local shear buckling of thin-walled cassette infilled by rigid insulation*, Journal of Constructional Steel Research, 60 (3–5), Mar-May 2004, 581–599.
- [8] Dubina D., Ungureanu V. and Landolfo R., *Design of Cold-formed Steel Structures*, ECCS 2012, Ernst & Sohn.
- [9] <https://pruszynski.com.pl/kaseta-scienna-600-120,prod,79,1750.php>(access:19.07.2018).
- [10] <http://termolan.pt/en/solutions/industrial-buildings> (access: 19.07.2018).
- [11] König J., *Transversally loaded thin-walled C-shaped panels with intermediate stiffeners*, Swedish Council for Building Research, Stockholm 1978, Sweden.
- [12] PN-EN 1993-1-3:2008. Eurokod 3. Projektowanie konstrukcji stalowych. Część 1-3: Reguły ogólne. Reguły uzupełniające dla konstrukcji z kształtowników i blach profilowanych na zimno.
- [13] PN-EN 1993-1-5:2008. Eurokod 3. Projektowanie konstrukcji stalowych. Część 1-5: Blachownice.
- [14] Program AutoCAD 2017 wersja edukacyjna.
- [15] Program Mathcad 14.
- [16] Program Microsoft Excel 2010.
- [17] Pięciorak E., Piekarczyk M., *Wyznaczanie efektywnego przekroju zginanej blachy trapezowej w ujęciu normy PN-EN 1993-1-3*, Czasopismo Techniczne, R. 109 z. 20. Budownictwo 2012 3-B, s. 113–137.
- [18] Pięciorak E., *The influence of support widths of trapezoidal sheets on local transverse resistance of the web according to PN-EN 1993-1-3*, Czasopismo Techniczne, R. 111 z. 12. Budownictwo 2014 4-B, s. 47–57.
- [19] Thomasson J., *Thin-Walled C-Shaped Panels in Axial Compression*, Swedish Council for Building Research, Stockholm 1978, Sweden.
- [20] Vyberg G., *Diaphragm action of assembled C-Shaped Panels*, Swedish Council for Building Research, Stockholm 1976, Sweden.

If you want to quote this article, its proper bibliographic entry is as follow: Pięciorak E., Piekarczyk M., Ciurej H., Betlej M., *The determination of moment resistance for a liner tray restrained by sheeting according to european standard PN-EN 1993-1-3*, Technical Transactions, Vol. 12/2018, pp. 77–94.